A roadmap for vortex particle accelerators

Dmitry Karlovets

ITMO University, St. Petersburg
Institute of Modern Physics, CAS



commons.wikimedia.org

Chirality 2026
Zhuhai, China
17 November 2026

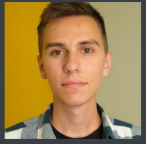
Research group at ITMO University



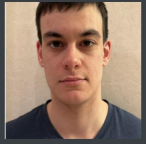
Alisa Chaikovskaia
Postdoc



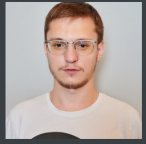
Alexander Dyatlov
PhD student



Alexander Shchepkin
PhD student



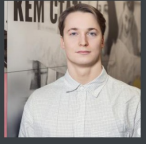
Timofey Panfilov
PhD student



Dmitriy Grosman
PhD student



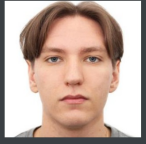
Ilia Pavlov
PhD student



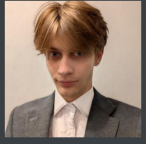
Maxim Maximov
PhD student



Daria Kargina
Student



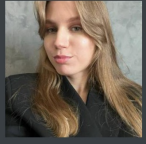
Anton Murtazin
Student



Dmitrii Protan
Student



Anton Tarantin
PhD student



Diana Myslyaeva
Invited lecturer

physics.itmo.ru/en/research-group/5430

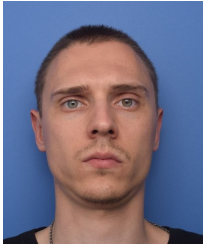
Our collaborators at JINR

Joint Institute for Nuclear Research

Dzhelepov Laboratory of Nuclear Problems



Mikhail Nozdrin



Konstantin Popov



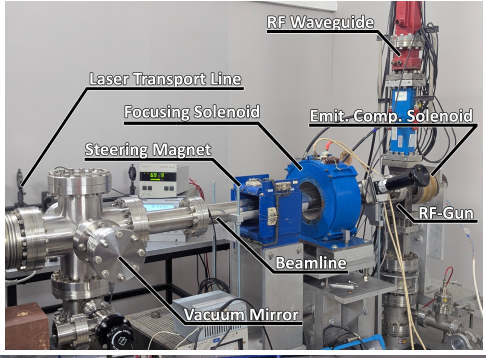
Valery Kobets



Dmitry Naumov

dlnp.jinr.ru/en

JINR: experimental development underway

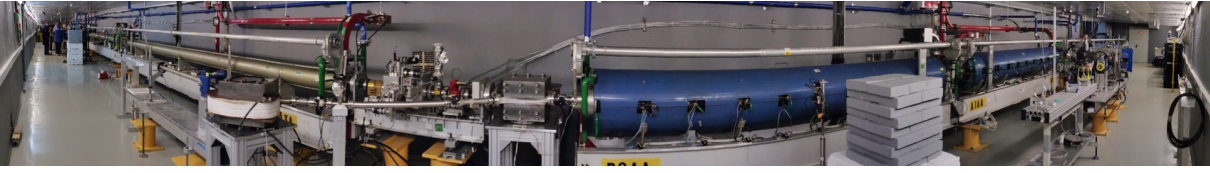


Electron photogun

5 MeV

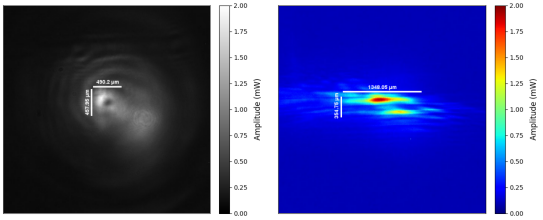
LINAC-200

$200\,\text{MeV} \xrightarrow{2027} 400\,\text{MeV}$



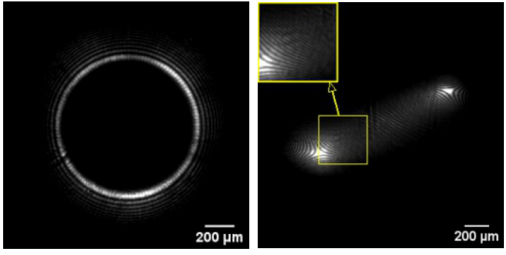
UV vortices in the JINR laser

2025 262 nm $\ell = 1$



Spiral zone plate

2026 266 nm $\ell = 64$



Spiral phase plate

Cylindrical lens: $|\ell| + 1$ lobes (2 and 65)

Next: transfer OAM to photoelectrons

Dyatlov et al., Appl. Opt. (2025)
Opt. Commun. (2026)

Appl. Opt.

Opt. Commun. 2026

High energy $\longrightarrow$ nuclear and particle channels

The quantum state enters the scattering probability

Plane waves

$$d\sigma^{(\mathrm{pw})} \propto |M_{fi}^{(\mathrm{pw})}|^2$$

Wave packets

$$\boxed{d\sigma_{\mathrm{gen}} = \frac{dW}{L}}$$

dW: scattering probability L: luminosity $(\hbar = c = 1)$

$$dW = \int \frac{d^3p_1\, d^3p_2\, d^3k}{(2\pi)^9}\, \mathcal{L}(\mathbf{p}_i, \mathbf{k})\, d\sigma(\mathbf{p}_i, \mathbf{k})$$

$$d\sigma(\mathbf{p}_i, \mathbf{0}) = d\sigma^{(\mathrm{pw})}(\mathbf{p}_i)$$

Karlovets, JHEP (2017) Karlovets and Serbo, PRD (2020)

Colliding wave packets: Wigner functions

$$\mathcal{L}(\mathbf{p}_i, \mathbf{k}) = v(\mathbf{p}_i) \int d^4x\, d^3R\, e^{i\mathbf{k}\cdot\mathbf{R}}\, n_1(\mathbf{r}, \mathbf{p}_1, t)\, n_2(\mathbf{r}+\mathbf{R}, \mathbf{p}_2, t)$$

Wigner function of wave packet 1

Wigner function of wave packet 2

$$n_i(\mathbf{r}, \mathbf{p}, t) = \int d^3y\, e^{-i\mathbf{p}\cdot\mathbf{y}} \psi_i^*(\mathbf{r}-\mathbf{y}/2, t)\psi_i(\mathbf{r}+\mathbf{y}/2, t)$$

$$v(\mathbf{p}_i) = \frac{\sqrt{(p_{1\mu}p_2^\mu)^2 - m_1^2 m_2^2}}{\varepsilon_1 \varepsilon_2} \qquad d^4x = dt\, d^3r \qquad (\hbar = c = 1)$$

Packet size, phase and overlap affect the cross section

Karlovets and Serbo, Phys. Rev. D 101, 076009 (2020)

First correction to the plane-wave result

Narrow packets, smooth amplitude: $\delta p \ll m \quad (\hbar = c = 1)$

$$d\sigma_{\rm gen} = d\sigma^{\rm incoh} + d\sigma^{\rm int} + \mathcal{O}\Big((\delta p)^2\Big)$$

$d\sigma^{\rm incoh}$: plane-wave cross section averaged over incident momenta

$$d\sigma^{\rm int} = -\frac{1}{L}\int \frac{d^3p_1\, d^3p_2}{(2\pi)^6}\, d^4x\, v(\mathbf{p}_i)\, n_1\, \frac{\partial n_2}{\partial \mathbf{r}}\, d\sigma^{(\rm pw)}(\mathbf{p}_i)\, \partial_{\Delta\mathbf{p}}\zeta_{fi}^{(\rm pw)}(\mathbf{p}_i)$$

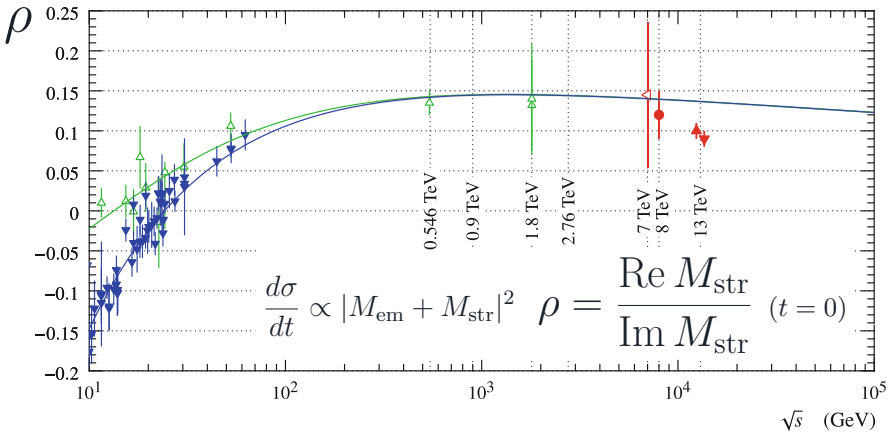
$$M_{fi}^{(\rm pw)} = |M_{fi}^{(\rm pw)}| e^{i\zeta_{fi}^{(\rm pw)}}, \qquad \partial_{\Delta\mathbf{p}} = \frac{\partial}{\partial \mathbf{p}_1} - \frac{\partial}{\partial \mathbf{p}_2}$$

$$n_i = n_i(\mathbf{r}, \mathbf{p}_i, t) \qquad d^4x = dt\, d^3r$$

The correction probes the momentum dependence of the phase.

Karlovets and Serbo, Phys. Rev. D 101, 076009 (2020) Karlovets, JHEP 03 (2017) 049

Scattering phases: the TOTEM example



Data

- TOTEM
- ▼ pp
- △ $\bar{p}p$

13 TeV

$\rho = 0.09 \pm 0.01$
or 0.10 ± 0.01

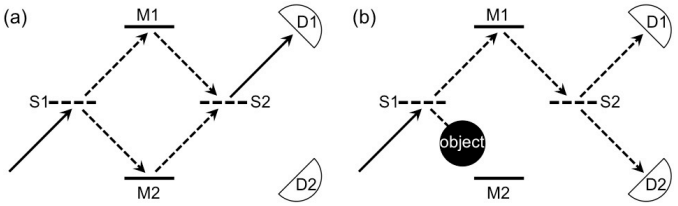
TOTEM 2019

- **COMPETE**: pre-LHC fits (curves)

Wave packets probe the momentum dependence of the phase.

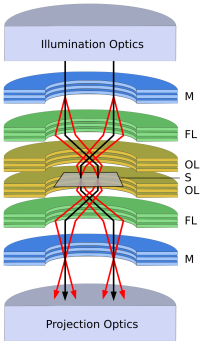
TOTEM, EPJ C (2019) COMPETE, PRD (2002) West and Yennie, Phys. Rev. (1968)

Electron microscopy



- **Interaction-free detection**

  Lower dose, less damage



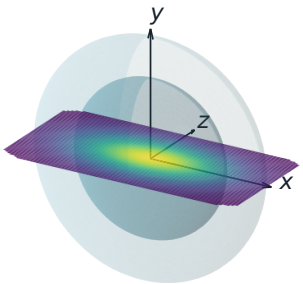
- **Multi-pass microscopy**

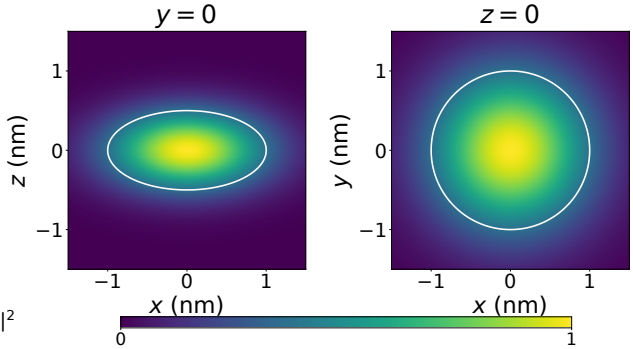
  Phase and state control

Elitzur and Vaidman, Found. Phys. (1993) Kruit et al., Ultramicroscopy (2016)
Turner et al., PRL (2021) Juffmann et al., Sci. Rep. (2017)

An electron wave packet at the source

Model packet $\rho = 1$ nm $\Delta z = 0.5$ nm





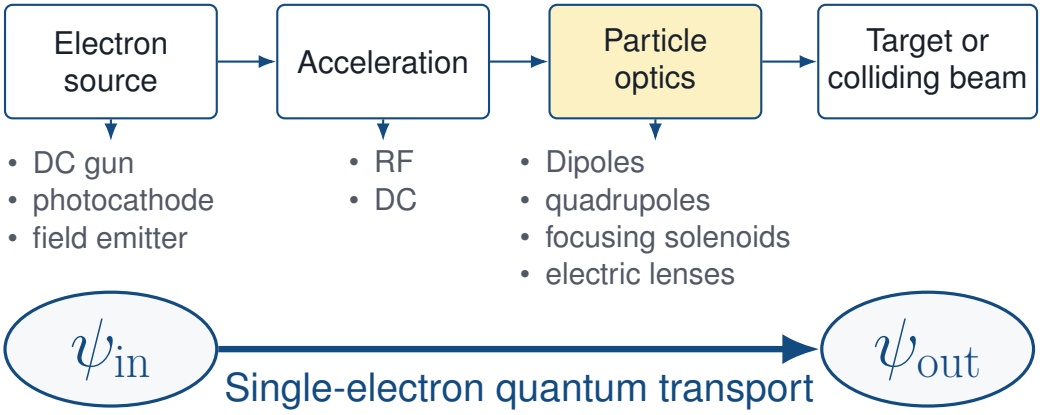
$$|\psi|^2 \propto e^{-(x^2+y^2)/\rho^2 - z^2/\Delta z^2}$$

$$\rho = \sqrt{\langle x^2 + y^2 \rangle}, \quad \sqrt{\langle z^2 \rangle} = \Delta z/\sqrt{2}$$

Nanometres at the source $\xrightarrow{\text{propagation and focusing}}$ micrometres at a magnet

Ehberger et al., PRL (2015) Johnsson et al., PRL (2005)

From source to target



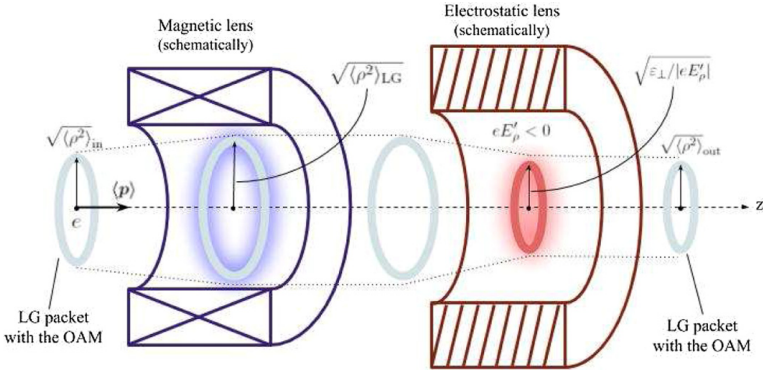
D. Karlovets et al., arXiv:2611.08010 (2026)

2611.08010

Axial symmetry preserves canonical OAM

Acceleration and focusing with axial symmetry

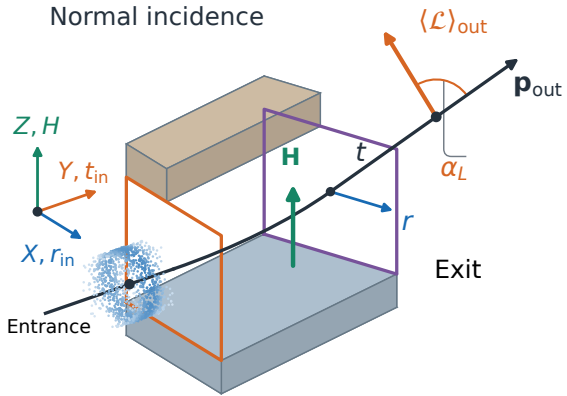
$$\hat{L}_z^{\mathrm{can}} = -i\hbar\partial_\varphi, \qquad [\hat{\mathcal{H}}(t), \hat{L}_z^{\mathrm{can}}] = 0 \quad \Longrightarrow \quad \boxed{\ell_{\mathrm{out}} = \ell_{\mathrm{in}}}$$



D. Karlovets, New J. Phys. (2021)

NJP 2021

OAM after a dipole



$\theta = 20^\circ$ $\quad L_{\text{mag}} = \rho\theta = 0.4$ m

Packet centre

$$\mathbf{r}_c = \langle\hat{\mathbf{r}}\rangle, \quad \boldsymbol{\pi}_c = \langle\hat{\boldsymbol{\pi}}\rangle$$

$$\delta\hat{A} = \hat{A} - \langle\hat{A}\rangle$$

$$\boxed{\hat{\boldsymbol{\mathcal{L}}} = \delta\hat{\mathbf{r}} \times \delta\hat{\boldsymbol{\pi}}}$$

Intrinsic kinetic OAM

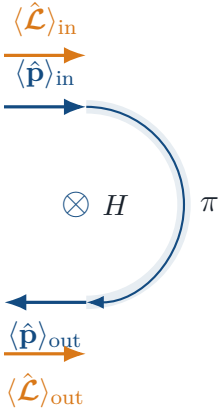
$$W = \frac{\Delta\mathcal{L}_{\parallel}}{|\langle\hat{\boldsymbol{\mathcal{L}}}\rangle|}$$

OAM spread along $\langle\hat{\boldsymbol{\mathcal{L}}}\rangle$

Entrance rest frame: $R_\perp = \sqrt{\langle\delta x^2 + \delta z^2\rangle}, \quad R_\parallel = \sqrt{\langle\delta y^2\rangle}$

D. Karlovets et al., arXiv:2611.08010 (2026)

Mean OAM after the magnet



$$\langle\hat{\mathcal{L}}_r\rangle_{\rm out} = \tfrac{1}{2}\gamma\ell\hbar\sin\theta$$

$$\langle\hat{\mathcal{L}}_t\rangle_{\rm out} = \ell\hbar(\cos\theta + \tfrac{1}{2}\theta\sin\theta)$$

At a half turn: $\langle\hat{\mathcal{L}}_t\rangle_{\rm out} = -\ell\hbar$

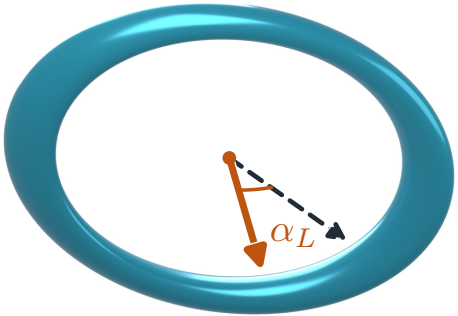
$$\langle\hat{\mathcal{L}}_H\rangle_{\rm out} = 0 \quad \Longleftarrow \quad \langle(\delta\hat{p}_r^{(0)})^2\rangle = \langle(\delta\hat{p}_t^{(0)})^2\rangle$$

Mean OAM can reverse with a broad spectrum

D. Karlovets et al., arXiv:2611.08010 (2026)

2611.08010

A 5° bend can tilt OAM by 23.6°



Spatio-temporal vortex

$\longrightarrow \langle \hat{\boldsymbol{\mathcal{L}}} \rangle$ $\dashrightarrow \langle \hat{\mathbf{p}} \rangle$

D. Karlovets et al., arXiv:2611.08010 (2026)
Bliokh and Nori, Phys. Rev. A 86, 033824 (2012)

IMP beamline

$$\alpha_L = 23.6^\circ$$

$$W = 12\%$$

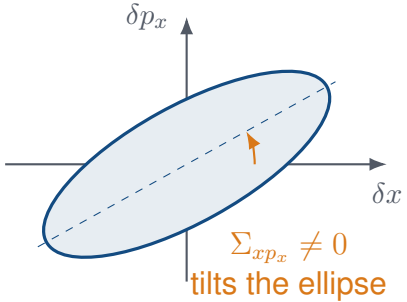
$$K = 4.6 \text{ MeV}$$

$$H = 5 \text{ mT}, \quad \ell = 64$$

$$(R_\perp, R_\parallel) = (2, 0.2)\,\mu\text{m}$$

2611.08010

Normalized emittance of a single wave packet



Covariance matrix

$$\Sigma_x = \begin{pmatrix} (\Delta x)^2 & \Sigma_{xp_x} \\ \Sigma_{xp_x} & (\Delta p_x)^2 \end{pmatrix}$$

Packet size, momentum spread, correlation

$$\Sigma_{xp_x} = \tfrac{1}{2}\langle \delta\hat{x}\delta\hat{p}_x + \delta\hat{p}_x\delta\hat{x} \rangle$$

$$\varepsilon_{n,x} = \frac{\sqrt{\det \Sigma_x}}{mc} \geq \frac{\hbar}{2mc}$$

Normalized emittance

$$(\Delta x)^2(\Delta p_x)^2 - \Sigma_{xp_x}^2 \geq \hbar^2/4$$

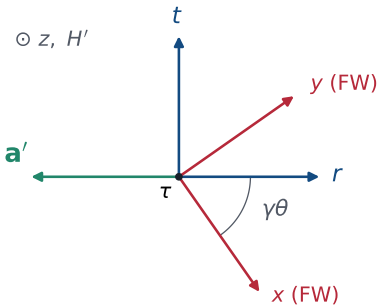
Robertson–Schrödinger relation

Karlovets, New J. Phys. (2021) Robertson, Phys. Rev. (1934)

NJP 2021

Different clock rates across the packet

τ: proper time at the packet centre



Nonrotating axes at the centre (Fermi–Walker)

Clocks at fixed displacement $\delta\mathbf{r}$

$$\mathrm{d}t_{\mathrm{loc}} = N\,\mathrm{d}\tau$$

$$N = 1 + \frac{\mathbf{a}' \cdot \delta\mathbf{r}}{c^2}$$

$\delta\mathbf{r}$: position relative to the centre

$\mathbf{a}'$: centre's proper acceleration

Roura, PRX (2020). D. Karlovets et al., arXiv:2611.08010 (2026)

From the lab Hamiltonian to comoving evolution

$$\mathcal{H}_{\rm lab} = \sqrt{m^2c^4 + c^2\boldsymbol{\pi}^2} - e\Phi, \qquad \boldsymbol{\pi} = \mathbf{p} + e\mathbf{A}$$

Comoving frame: expansion to second order

$$i\hbar\partial_\tau \psi(\delta\mathbf{r},\tau) = \underbrace{\left[\frac{(\delta\hat{\boldsymbol{\pi}})^2}{2m} - \frac{m}{2c^2}(\mathbf{a}'\cdot\delta\hat{\mathbf{r}})^2\right]}_{\hat{\mathcal{H}}_2} \psi(\delta\mathbf{r},\tau)$$

τ: centre's proper time

$$\eta_{\rm NR} = \frac{\sqrt{\langle(\delta\hat{\boldsymbol{\pi}})^2\rangle}}{mc} \ll 1$$

$$\eta_a = \frac{|\mathbf{a}'|R_a}{c^2} \ll 1$$

R_a: rms size along $\mathbf{a}'$

Obukhov, Silenko and Teryaev, PRD (2013). D. Karlovets et al., arXiv:2611.08010 (2026)

Maslov's method: Heisenberg operators

$$\delta\hat{Z} = (\delta\hat{\mathbf{r}}, \delta\hat{\mathbf{p}})^T$$

$\mathbf{p}$: canonical momentum

$$\hat{\mathcal{H}}_2 = \frac{1}{2}\delta\hat{Z}^T G(\tau)\delta\hat{Z}$$

$$G_{AB}(\tau) = \left.\frac{\partial^2 \mathcal{H}_{\text{eff}}}{\partial Z_A\, \partial Z_B}\right|_{\text{centre}}$$

$\mathcal{H}_{\text{eff}}$: comoving Hamiltonian

G: a 6×6 matrix

for spreading, focusing and deformation

$$\frac{\mathrm{d}\delta\hat{Z}}{\mathrm{d}\tau} = \frac{i}{\hbar}[\hat{\mathcal{H}}_2, \delta\hat{Z}] = JG\,\delta\hat{Z}$$

$$J = \begin{pmatrix} 0 & I_3 \\ -I_3 & 0 \end{pmatrix}$$

Linear evolution of position and momentum

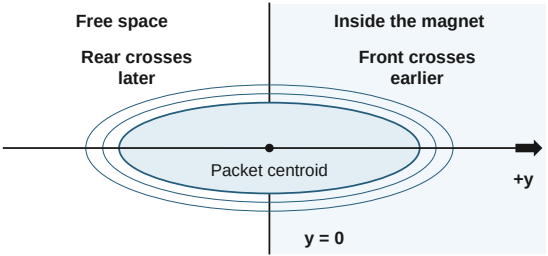
V. P. Maslov, *The Complex WKB Method for Nonlinear Equations I: Linear Theory*
Birkhäuser, Basel (1994), Progress in Mathematical Physics, vol. 16.
Bagrov, Belov and Trifonov, J. Phys. A (1993), Ann. Phys. (1996)



JPA 1993 Ann. Phys. 1996

Crossing a sharp boundary: a non-instantaneous process

Gauge-invariant kinetic moments are continuous at each crossing.



$$\langle \hat{\mathbf{r}} \rangle_{\times}^{+} = \langle \hat{\mathbf{r}} \rangle_{\times}^{-},$$
$$\langle \hat{\boldsymbol{\pi}} \rangle_{\times}^{+} = \langle \hat{\boldsymbol{\pi}} \rangle_{\times}^{-},$$
$$\Sigma_{\mathrm{kin},\times}^{+} = \Sigma_{\mathrm{kin},\times}^{-}.$$

$\pm$: limits at the same crossing

Σ_{kin}: covariance matrix of $(\hat{\mathbf{r}}, \hat{\boldsymbol{\pi}})$

- Finite force $\Rightarrow$ zero impulse at an instantaneous crossing.

D. Karlovets et al., arXiv:2611.08010 (2026)

Momentum shear in the linear approximation

Entrance rest frame: x radial, y along the orbit, z along $\mathbf{H}$

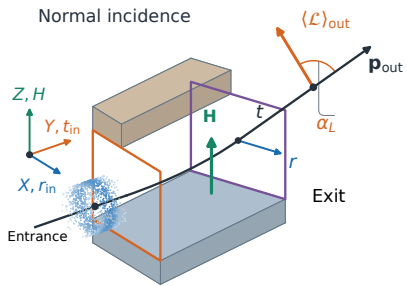
$$y + vt' = 0, \qquad t'_\times(y) = -y/v$$

$$H' = \gamma H, \quad E'_x = vH', \quad q = -e$$

$$\Delta\pi_x(y) = \int_{-y/v}^{0} (-eE'_x)\,\mathrm{d}t' = -eH'y$$

$$\boxed{\begin{aligned}\delta\hat{\pi}_x^+ &= \delta\hat{p}_x^- - eH'\delta\hat{y},\\ \delta\hat{\pi}_y^+ &= \delta\hat{p}_y^-.\end{aligned}}$$

$$\frac{\mathrm{d}\hat{\boldsymbol{\pi}}}{\mathrm{d}t'} = -e\mathbf{E}' - \frac{e}{2m}\left(\hat{\boldsymbol{\pi}}\times\mathbf{H}' - \mathbf{H}'\times\hat{\boldsymbol{\pi}}\right).$$



At $t' = 0$: $-$ free solution, $+$ solution in the field

D. Karlovets et al., arXiv:2611.08010 (2026)

Entrance matching phase

In the symmetric gauge

$$\mathbf{A}' = \frac{H'}{2}(-\delta y, \delta x, 0), \qquad \delta\hat{\boldsymbol{\pi}} = \delta\hat{\mathbf{p}} + e\mathbf{A}'$$

$$\delta\hat{p}_x^+ = \delta\hat{p}_x^- - \frac{eH'}{2}\delta\hat{y}, \qquad \delta\hat{p}_y^+ = \delta\hat{p}_y^- - \frac{eH'}{2}\delta\hat{x}$$

An added phase $\chi/\hbar$ shifts momentum: $\Delta\mathbf{p} = \nabla\chi$

$$\psi^+(\delta\mathbf{r}, t' = 0) = \exp\left[-\frac{ieH'}{2\hbar}\delta x\delta y\right]\psi^-(\delta\mathbf{r}, t' = 0)$$

ψ^-: free solution ψ^+: solution in the field

D. Karlovets et al., arXiv:2611.08010 (2026)

Transport of sizes and correlations

$$\Sigma_{ab} = \frac{1}{2}\langle \delta\hat{Z}_a \delta\hat{Z}_b + \delta\hat{Z}_b \delta\hat{Z}_a \rangle$$

Σ: position and momentum covariances



$$S = C_{\rm out} S_{\rm bulk} C_{\rm in}, \qquad \delta\hat{Z}_{\rm out} = S\delta\hat{Z}_0$$

$$\boxed{\Sigma_{\rm out} = S\Sigma_0 S^T}$$

- Mean OAM: second moments.
- OAM variance: fourth moments.

D. Karlovets et al., arXiv:2611.08010 (2026)

Generalized BMT equation

Kinetic OAM in the packet rest frame

$$\frac{\mathrm{d}}{\mathrm{d}\tau}\langle\hat{\boldsymbol{\mathcal{L}}}\rangle = \frac{e}{2m}\mathbf{H}' \times \langle\hat{\boldsymbol{\mathcal{L}}}\rangle + \underbrace{\mathbf{K}_\pi}_{\text{deformation}} + \underbrace{\mathbf{K}_a}_{\text{acceleration}}$$

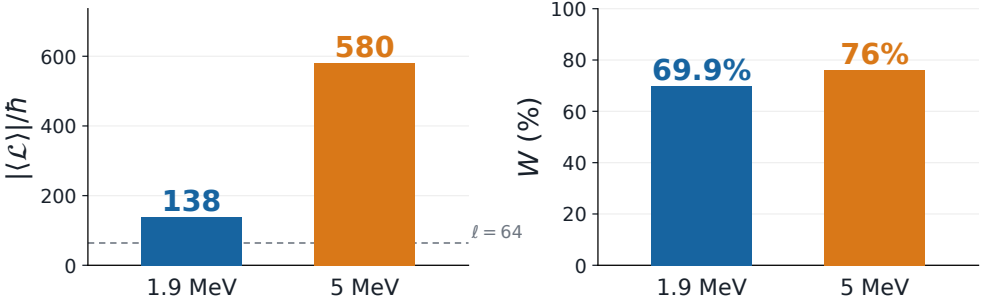
Packet shape and correlations enter OAM transport.

- $\mathbf{K}_\pi$, $\mathbf{K}_a$ can change the OAM magnitude $\Rightarrow$ direction and magnitude evolve.
- Uniform field, same initial state:
  Lin, Ji et al.: same dynamics.
  Gallatin–McMorran: same OAM variance.
- Silenko–Zhang–Zou: laboratory dynamics, including acceleration.

Gallatin and McMorran, PRA 86, 012701 (2012)
Y. Lin, L. Ji et al., arXiv:2611.04162 (2026)
Silenko et al., PRL (2017), PRL (2018) D. Karlovets et al., arXiv:2611.08010 (2026)

JINR photoinjector

28.5° bend $\rho = 0.55$ m $H = 14.3/33.3$ mT



After exit $\ell_{\text{in}} = 64, \quad (R_\perp, R_\parallel) = (3, 0.3)\,\mu$m

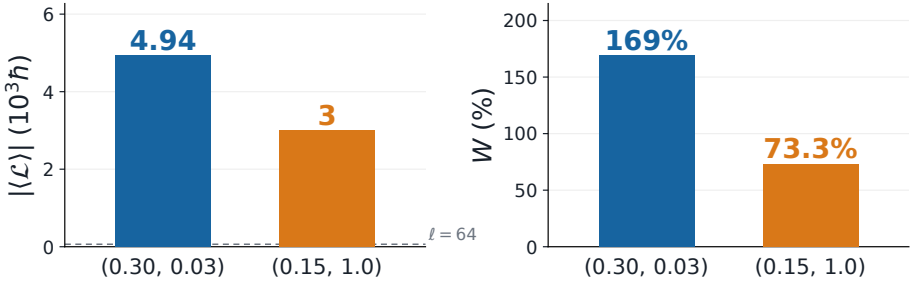
Test OAM tilt and broadening

D. Karlovets et al., arXiv:2611.08010 (2026)

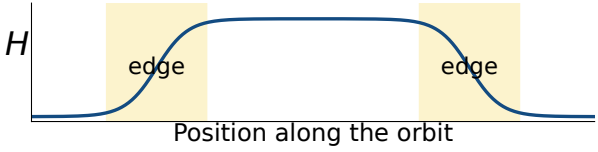
2611.08010

LINAC-200: packet size matters

$K = 30$ MeV $35°$ bend $\rho = 0.532$ m $H = 191$ mT



After exit $(R_\perp, R_\parallel)$ in μm $\ell_{\rm in} = 64$



Logistic field edges

Incidence spread: 0.3 mrad

D. Karlovets et al., arXiv:2611.08010 (2026)

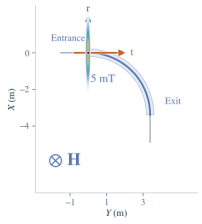
Laboratory probability density: initial $\ell = 0$ (Gaussian packet)

Equal laboratory time

At the entrance

$t_{\mathrm{lab}} = 0$ ns • bend 0°

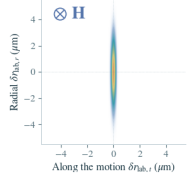
(a) Trajectory and longitudinal section



Section enlarged by a constant factor of 450 000.

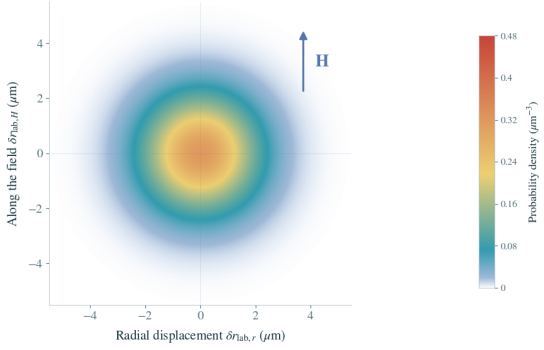
(b) Central longitudinal section

In the orbital plane, $\delta r_{\mathrm{lab},H} = 0$



(c) Central transverse section

Perpendicular to the velocity, $\delta r_{\mathrm{lab},t} = 0$



Fixed spatial and density scales

rms widths (μm)	Radial (r)	Along H
Whole packet	1.414	1.414
Transverse section	1.414	1.414

Electron • K = 4.6 MeV • H = 5 mT • bend 90° • initial $\ell = 0$ • rest-frame waist: R⊥ = 2 μm, R∥ = 1 μm

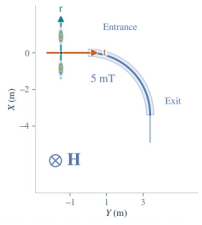
Laboratory probability density: initial $\ell = 10$

Equal laboratory time

Before the magnet

$t_{\mathrm{lab}} = -5.001$ ns • bend 0°

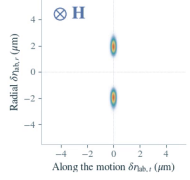
(a) Trajectory and longitudinal section



Section enlarged by a constant factor of 450 000.

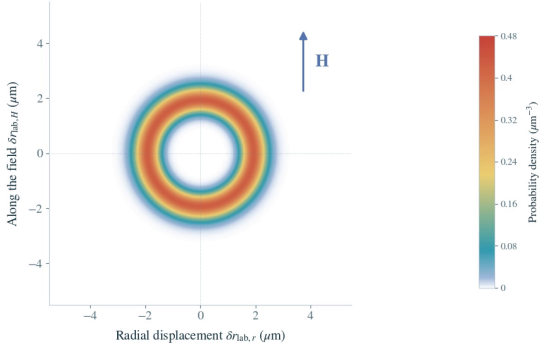
(b) Central longitudinal section

In the orbital plane, $\delta r_{\mathrm{lab},H} = 0$



(c) Central transverse section

Perpendicular to the velocity, $\delta r_{\mathrm{lab},t} = 0$



Fixed spatial and density scales

rms widths (μm)	Radial (r)	Along H
Whole packet	1.432	1.432
Transverse section	1.432	1.432

Electron • K = 4.6 MeV • H = 5 mT • bend 90° • initial $\ell = 10$ • rest-frame waist: R⊥ = 2 μm, R∥ = 1 μm

A vortex electron in a magnetic field

One in-field turn: the effect of the reference-orbit acceleration potential

IDEALIZED ORBIT · MIRRORCLE-6X K AND ρ

K = 6 MeV · H = 144 mT · ρ = 15 cm · ℓ = 64 · R⊥ = 1 μm · R∥ = 0.2 μm

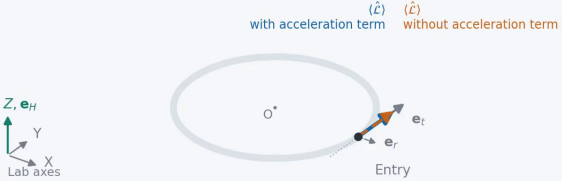
ORBIT AND MEAN KINETIC OAM

Lab orbit · rest-frame arrows

$\langle\hat{\mathcal{L}}\rangle = \langle\delta\hat{\mathbf{r}} \times \delta\hat{\boldsymbol{\pi}}\rangle$

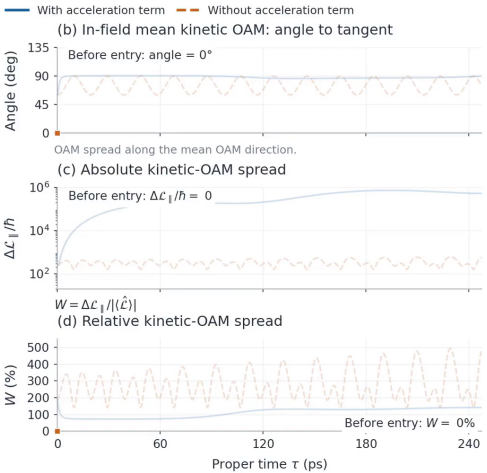
Orbital axes r, t, H

Before entrance (τ = 0⁻): OAM along the tangent



ACCELERATION TERM	$\lvert\langle\hat{\mathcal{L}}\rangle\rvert/\hbar$	W (%)
Included	64	0
Omitted	64	0

Arrows: direction only; lengths are not to scale



Pale curves: later times. No exit matching.

Before entrance, the mean kinetic OAM points along the mean momentum.

A smaller relative width W can accompany a much larger absolute OAM spread.

Playback follows the waltz; the counters show physical time.

OAM after N turns

Uniform field

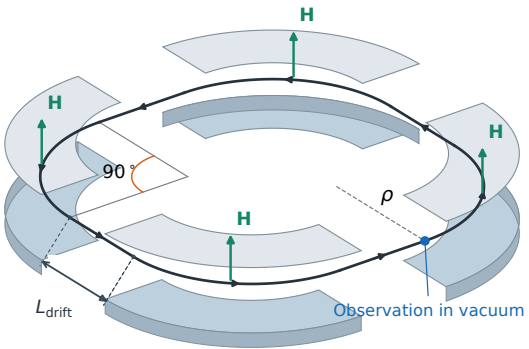
After N full turns, in vacuum

$$\langle \hat{\mathcal{L}}_t \rangle_N = \ell\hbar$$

$$(\Delta\mathcal{L}_t)^2 = \left(\frac{2\pi N}{eH}\right)^2 \times \langle (\delta\hat{p}_r^{(0)})^2 (\delta\hat{p}_H^{(0)})^2 \rangle$$

$$\boxed{(\Delta\mathcal{L}_t)^2 \propto N^2}$$

Four 90° dipoles + drifts

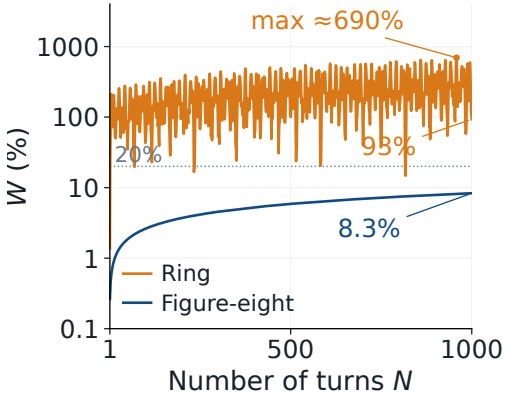


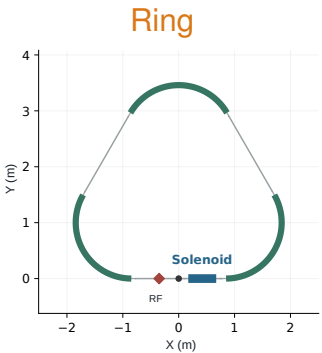
D. Karlovets et al., arXiv:2611.08010 (2026)

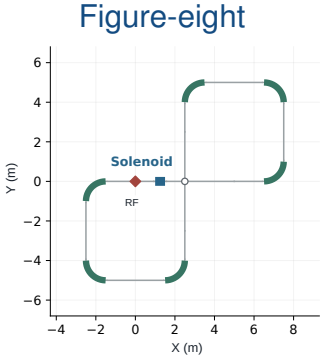
2611.08010

1000 turns: preliminary OAM width

20 MeV $\ell = 64$ $\rho = 1$ m Linear optics + local photon recoil







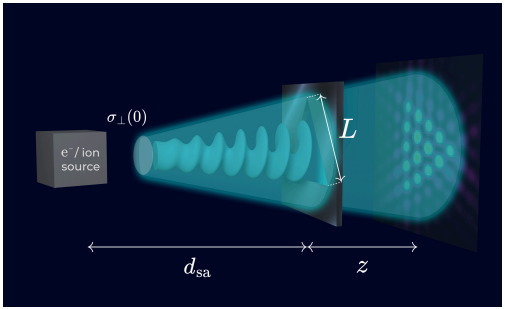
W: instantaneous rest-frame OAM width $W(0) = 0$

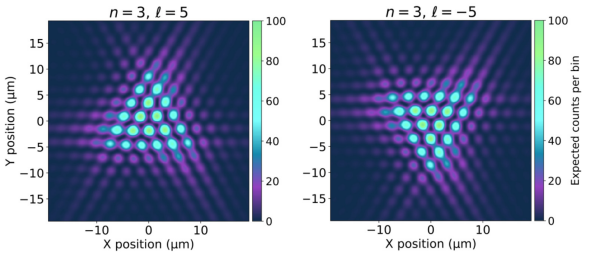
Roadmap: beamlines and linacs

Method / task	Theoretical tools needed	Experiments needed
1 Preparation of vortex electrons		
• Photoemission with twisted light	• **Done** [1]	• Vortex emission at low current
• Electrostatic chopsticks	• **Done** [2]	• **Done**: 300 keV [2] • Refine for other sources/machines
• Magnetized cathodes	• **Done** [3]	• Classical beams: **done** [4] • Single-electron OAM at low current
2 Diagnostics		
• Triangular apertures • Focusing optics	• MeV diffraction: **done** [5]	• **Done**: 300 keV [6] • MeV tests
• Full quantum tomography	• MeV protocol needed	• Longitudinal state [7] • OAM with priors [8] • Full MeV tomography
3 OAM measurements and quantum tomography		
• Bending magnets • Quadrupoles	• Dipoles: **done** [9] • Focusing + tomography	• OAM before and after magnets

[1] Shchepkin & Karlovets, arXiv (2026) [2] Tavabi et al., APL (2022) [3] Karlovets, NJP (2021)
[4] Sun et al., PRSTAB (2004) [5] Maksimov et al., PRA (2025) [6] Guzzinati et al., PRA (2014)
[7] Fang et al., arXiv (2026) [8] Tavabi et al., arXiv (2026) [9] Karlovets et al., arXiv:2611.08010 (2026)

OAM retrieval from diffraction on triangular apertures





$E_{\mathrm{kin}} = 1$ MeV $\quad n = 3, \ell = \pm 5$

Aperture side: $L = 400$ nm $\quad$ Waist: $\sigma_\perp(0) = 10$ nm

Source $\rightarrow$ aperture: $d_{\mathrm{sa}} = 8$ cm $\quad$ Aperture $\rightarrow$ screen: $z = 1$ m

Radial rms divergence: $48\,\mu$rad

Opposite OAM gives mirrored patterns

Maksimov et al., PRA 112, 062823 (2025)

PRA 2025

Linear and Circular Accelerators

Method / task	Theoretical tools needed	Experiments needed
1 Vortex protons and ions: plans at IMP, Huizhou		
• Electrostatic chopsticks	• Adapt the electron model	• Prepare and measure OAM • Develop focusing solenoids • Image far-field diffraction
• Magnetized stripping foils	• Partly done [1]	• Classical GSI beams: **done** [2] • Single-particle OAM tests
2 Preserve the vortex state over many turns		
• Four dipoles + drifts	• **Done** [3] • Strong OAM spread • Focusing needed	• First: tomography at linacs and beamlines
• Ring and figure eight with focusing	• **In progress** • Full optics + realistic fringe fields • Relativistic transport	• After full-lattice modelling: • A concrete storage-ring proposal

Long far-field distances require focusing and diffraction imaging.

[1] Karlovets, NJP (2021) [2] Groening et al., PRL (2014)

[3] D. Karlovets et al., arXiv:2611.08010 (2026)

2611.08010

Steps in the near future

- Prepare relativistic vortex electrons at low current
  (Dubna: in progress)

  Next: control state degradation as current increases
- Measure OAM and its spectrum before and after a dipole
  (Dubna: next)
- MeV electron-state tomography (Dubna: next)
- Vortex ions and protons (IMP, Huizhou: planned)
- Circular accelerators and storage rings (long term)

Dilute beams: many particles, weak space charge, longer acquisition

D. Karlovets et al., arXiv:2611.08010 (2026)

Thank you

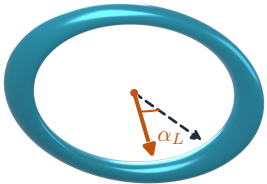


M. Nozdrin, K. Popov
V. Kobets, D. Naumov
X. Chen, S. Stafeev
A. Bogdanov, V. Gerasimov
A. Surzhykov, Y. Litvinov
K. Bliokh, I. Ivanov
L. Ji, P. Zhang, L. Zou
A. Silenko

and many colleagues

OAM tilt at IMP

After a 5° bend



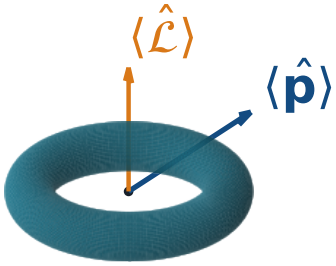
$\longrightarrow \langle \hat{\boldsymbol{\mathcal{L}}} \rangle$ $\dashrightarrow \langle \hat{\mathbf{p}} \rangle$

$\alpha_L = 23.6^\circ$ $W = 12\%$

$K = 4.6$ MeV $H = 5$ mT

$\ell = 64$, $(R_\perp, R_\parallel) = (2, 0.2)\,\mu$m

Spatiotemporal vortex

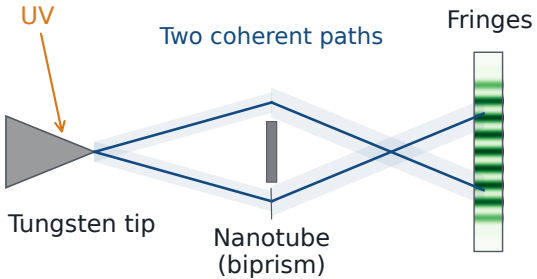


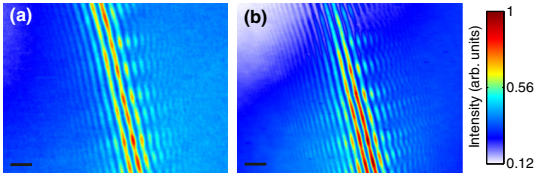
$$\arg \psi = \ell \arg[x - i(z - vt)]$$

D. Karlovets et al., arXiv:2611.08010 (2026)
Bliokh and Nori, PRA (2012)

PRA 2012 2611.08010

An electron's transverse size at emission





Photoemission: 44 eV DC: 53 eV

Source width from interference: $\rho \sim 1$ nm

0.80 nm (photoemission), 0.55 nm (DC)

Single-electron pulses: 30 keV 0.1 electron/pulse $I_{\mathrm{av}} = 0.041$ pA

Ehberger et al., PRL (2015)
Kirchner et al., NJP (2013)

PRL 2015 NJP 2013

Longitudinal size after photoemission

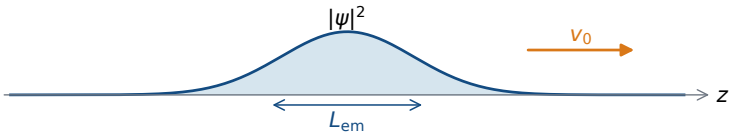
XUV light $\longrightarrow$ Ar atom $\longrightarrow$ electron packet

Packet duration

$\Delta t_{\mathrm{em}} = 180$–$260$ as

Kinetic energy

$K_0 \simeq 15$ eV



$v_0 \simeq 2.3$ nm/fs

$L_{\mathrm{em}} \sim v_0 \Delta t_{\mathrm{em}} \sim 0.4$–$0.6$ nm

Johnsson et al., PRL (2005)

PRL 2005

Position–momentum correlations carry OAM

Packet widths and correlations

$$\Sigma = \begin{pmatrix} \Sigma_{rr} & \Sigma_{rp} \\ \Sigma_{pr} & \Sigma_{pp} \end{pmatrix}$$

$$\delta\hat{\boldsymbol{\pi}} = \delta\hat{\mathbf{p}} + e\mathbf{A}'$$

With kinetic momentum

$$(C_{r\pi})_{ij} = \tfrac{1}{2}\langle\{\delta\hat{r}_i, \delta\hat{\pi}_j\}\rangle$$

$$\boxed{\langle\hat{\mathcal{L}}_i\rangle = \epsilon_{ijk}(C_{r\pi})_{jk}}$$

$$C_{r\pi} = M_\pi + \frac{C_{r\pi} - C_{r\pi}^T}{2}$$

Expansion and shear: M_π

Mean OAM: the antisymmetric part

$$\langle\hat{\mathcal{L}}_y\rangle = (C_{r\pi})_{zx} - (C_{r\pi})_{xz}$$

D. Karlovets et al., arXiv:2611.08010 (2026)

Weak-bend minimum

$$\gamma \gg 1, \quad \theta \sim \gamma^{-1}, \quad \ell > 0$$

$$\alpha_L \simeq \arctan \frac{\gamma\theta}{2} \qquad \frac{R_\perp}{R_\parallel} = \sqrt{2(|\ell| + 1)}$$

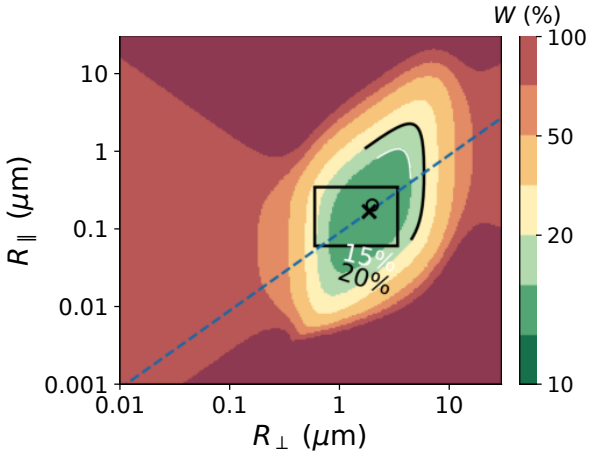
$$\boxed{W^2_{\min} = \frac{1}{2}\sin^4 \alpha_L + \frac{|\ell| + 2}{2\ell^2}\sin^2 \alpha_L}$$

$$|\ell| \gg 1, \quad W < 20\% \qquad \Longrightarrow \qquad \alpha_L \lesssim 32^\circ$$

Karlovets et al., arXiv:2611.08010 (2026)

2611.08010

IMP: packet sizes control the OAM width



$K = 4.6$ MeV

$H = 5$ mT

$\theta = 5^\circ$, $\ell = 64$

$R_\perp = 2\ \mu\mathrm{m}$

$R_\parallel = 0.2\ \mu\mathrm{m}$

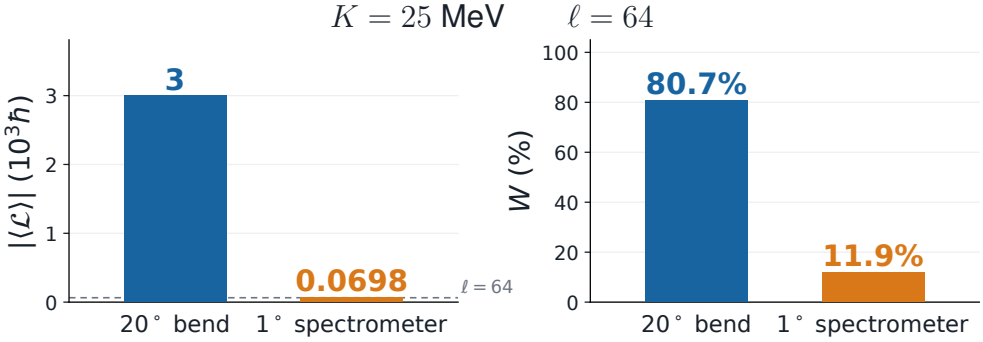
$W \simeq 12\%$

$\alpha_L \simeq 24^\circ$

$R_\parallel = 0.1 R_\perp$

D. Karlovets et al., arXiv:2611.08010 (2026)

BNL ATF: magnet and packet sizes



$H = 74.2$ mT $\quad L_{\rm mag} = 0.40$ m

$(R_\perp, R_\parallel) = (3, 0.3)\,\mu$m

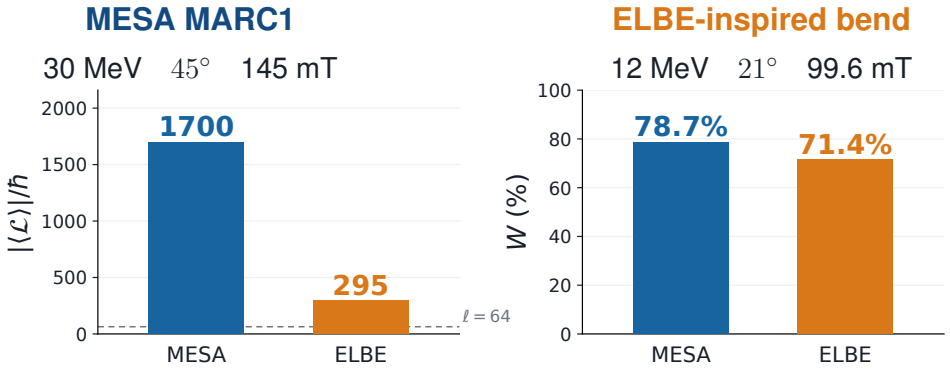
$H = 6.2$ mT $\quad L_{\rm mag} = 0.24$ m

$(R_\perp, R_\parallel) = (1.7, 0.15)\,\mu$m

2611.08010

D. Karlovets et al., arXiv:2611.08010 (2026)

Larger bends: MESA and ELBE

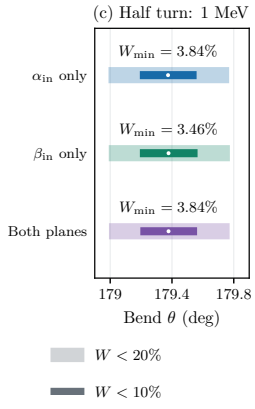


$\ell = 64 \qquad (R_\perp, R_\parallel) = (0.3, 1)\ /\ (0.45, 0.27)\ \mu\text{m}$

D. Karlovets et al., arXiv:2611.08010 (2026)

2611.08010

Half-turn tolerances



$K = 1$ MeV $\quad H = 5$ mT $\quad \ell = 10$

$(R_\perp, R_\parallel) = (10, 1)\,\mu$m

$\theta_* = 179.378^\circ, \quad W_{\min} = 3.84\%$

OAM width	$\pi - \theta$ (mrad)
$W < 20\%$	3.96–17.6
$W < 10\%$	7.63–14.0

Incidence: $\alpha_{\rm in}$ in-plane, $\beta_{\rm in}$ out-of-plane

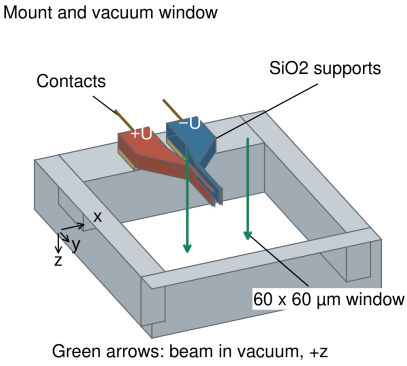
Fringe length 5 mm $\quad$ Angular spread 0.3 mrad per plane

Karlovets et al., arXiv:2611.08010 (2026)

2611.08010

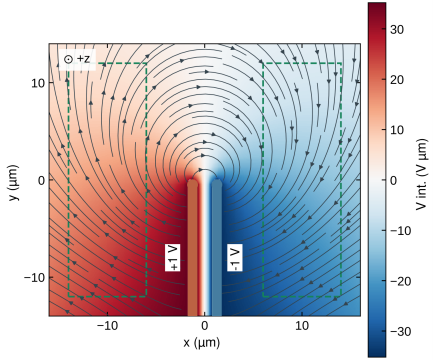
Electrostatic chopsticks

Electrode geometry



Green arrows: beam in vacuum, +z

Integrated potential V_{int}



Phase shift: $\chi = \dfrac{eV_{\mathrm{int}}}{\hbar v}$ $\quad V_{\mathrm{int}} = \int \Phi \, dz$ $\quad K = 1$–5 MeV

ITMO–JINR (2026) Tavabi et al., APL (2022)

APL 2022

Resolving the diffraction fringes

Lenses map angle to position: $R_{12} = \partial x_{\rm det}/\partial\theta_{\rm in}$

$$\Delta = \frac{2\lambda_{\rm dB}|R_{12}|}{\sqrt{3}\,L}$$

Target	$K = 1.5$ MeV	$K = 5$ MeV
Triangle side L	$4\,\mu$m	$2\,\mu$m
Effective $\lvert R_{12}\rvert$	270 m	380 m
Fringe spacing Δ	$50\,\mu$m	$50\,\mu$m

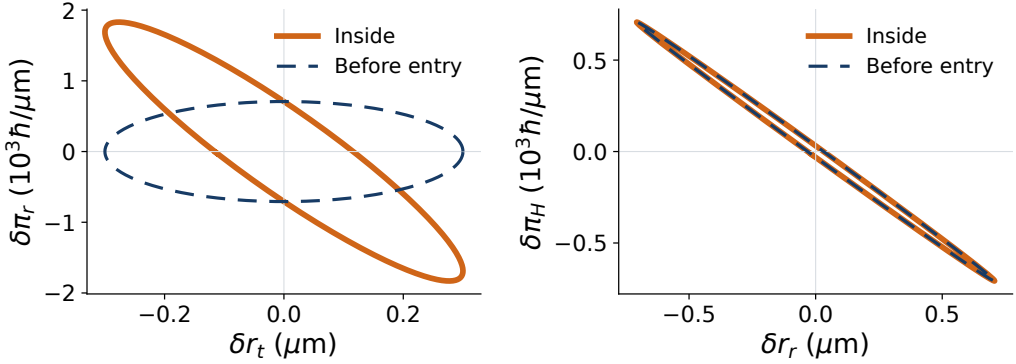
3–5-m line Detector resolution $\leq 10\,\mu$m

Maksimov et al., PRA (2025)

PRA 2025

The entrance shears the momentum distribution

$$\delta\hat{\pi}_r^+ = \delta\hat{p}_r^- - eB'\delta\hat{r}_t$$



$-/+$: before / inside the magnet B': rest-frame field

D. Karlovets et al., arXiv:2611.08010 (2026)

2611.08010

Population, density and acquisition time

Mean beamline population

$$\bar{N}_L = \frac{IL}{ev}$$

L: line length v: speed

$\bar{N}_L$ can exceed one.

Beam diagnostics

$$R_{\mathrm{det}} = \frac{I}{e} T\eta = f\bar{n}\, T\eta$$

T: transmission η: efficiency

f: pulse rate $\bar{n}$: particles / pulse

$$I = ef\bar{n}$$

Collisions: $R_{\mathrm{det}} = \mathcal{L}\,\sigma\eta$

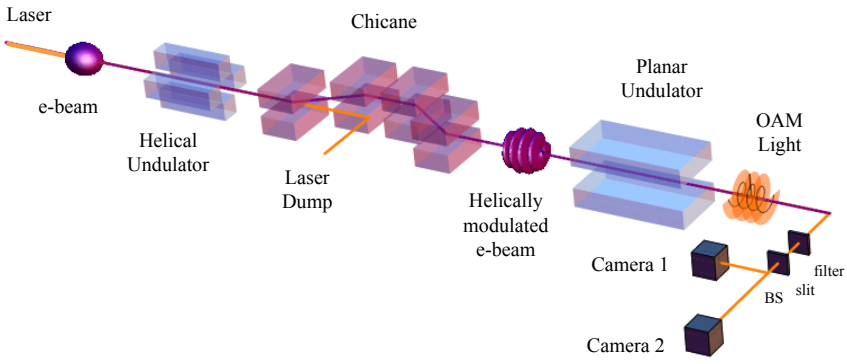
$\mathcal{L}$: luminosity σ: cross section

Local density and spacing control Coulomb perturbations.

For a pulsed beam, consider the density within each bunch.

D. Karlovets et al., arXiv:2611.08010 (2026)

Vortex X-rays at FELs



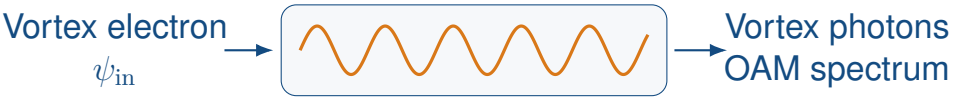
Helical density modulation at SLAC 15.6-nm vortices at FERMI

Goal: transfer single-electron OAM to X-rays

Hemsing et al., Nat. Phys. (2013)
Ribič et al., PRX (2017)

Nat. Phys. 2013 PRX 2017

Vortex electrons in a helical undulator



Circularly polarized wave

$$-i\hbar\partial_{\varphi_R}\psi = \ell\hbar\psi$$

Coordinates follow the quiver motion

Helical undulator

Calculate transport, emission and recoil over many periods

Then collective FEL gain

Goal: control photon OAM through the electron state

Karlovets, PRA (2012) Bogdanov et al., PRA (2018)
D. Karlovets et al., arXiv:2611.08010 (2026)

OAM and packet size inside a solenoid

$$\langle \hat{L}_z^{\rm can} \rangle = \ell\hbar, \qquad \langle \hat{L}_z^{\rm kin} \rangle = \ell\hbar - \frac{qH}{2}\langle \rho^2 \rangle$$

$q = -e$. The radius changes the kinetic OAM.

Packet widths and correlations (δ: deviation from the mean)

$$Q = \begin{pmatrix} \langle \delta\boldsymbol{\rho}^2 \rangle & \frac{1}{2c}\langle \delta\boldsymbol{\rho}\cdot\delta\mathbf{u}_\perp + \delta\mathbf{u}_\perp\cdot\delta\boldsymbol{\rho}\rangle \\ \frac{1}{2c}\langle \delta\boldsymbol{\rho}\cdot\delta\mathbf{u}_\perp + \delta\mathbf{u}_\perp\cdot\delta\boldsymbol{\rho}\rangle & \langle \delta\mathbf{u}_\perp^2\rangle/c^2 \end{pmatrix}$$

$$\varepsilon_{\rho,\rm eff} = \sqrt{\det \overline{Q}}$$

The bar averages oscillations in one focusing lens.

Karlovets, NJP (2021)

Packet sizes control the approximation

Entrance waist: $n = 0$, normal incidence

$R_\perp, R_\parallel$: rest-frame sizes $\qquad \lambda_C = \hbar/(mc)$

$$\eta^2_{\rm NR}(0^+) = \left[\frac{(|\ell|+1)\lambda_C}{R_\perp}\right]^2 + \left[\frac{\lambda_C}{2R_\parallel}\right]^2 + \left[\frac{\gamma e H R_\parallel}{mc}\right]^2$$

Momentum uncertainty and entrance shear

$$\eta_a(0^+) = \frac{(\gamma^2-1)R_\perp}{\sqrt{2}\,\rho}, \qquad \rho = \frac{\gamma m v}{eH}$$

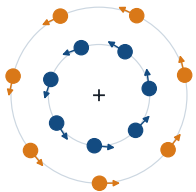
$$\boxed{(|\ell|+1)\lambda_C \ll R_\perp \ll \frac{\sqrt{2}\,\rho}{\gamma^2-1}}, \qquad \boxed{\frac{\lambda_C}{2} \ll R_\parallel \ll \frac{\rho}{\gamma\sqrt{\gamma^2-1}}}$$

Uncertainty sets the lower bounds, acceleration and shear the upper bounds.

D. Karlovets et al., arXiv:2611.08010 (2026)

Collective rotation and single-particle OAM

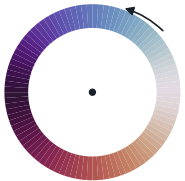
Collision system / beam



Noncentral collisions / magnetized beams

$$\mathbf{L}_{\text{system}} = \Sigma_a \, \mathbf{r}_a \times \mathbf{p}_a$$

Each particle's wave packet



Phase about the packet centre

$$\psi \propto e^{i\ell\varphi}, \quad L_z = \ell\hbar$$

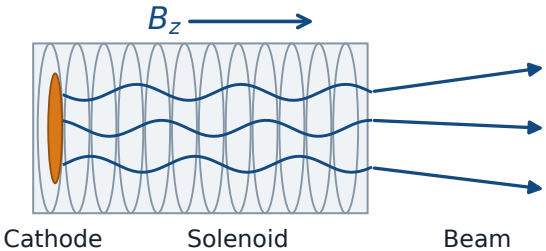
Free-space OAM mode, $\ell \in \mathbb{Z}$

Electrons, protons, neutrons, ions

Hadron: OAM of its centre-of-mass wave packet

STAR, Nature (2017) ALICE, PRC (2020) Karlovets, NJP (2021)

Magnetized beams: established technology



Classical angular-momentum-dominated beams

DESY–Fermilab
Magnetized electron sources

Fermilab A0 / FAST
Beam generation and manipulation

GSI / EMTEX
Ion stripping inside a solenoid

Quantum step: coherent preparation, low density, tomography

Edwards et al. (2000) Sun et al. (2004) Halavanau et al. (2018) Groening et al. (2014) Karlovets (2021)

Quantum transport theory came first



Semiclassical transport

Bagrov, Belov, Trifonov and collaborators

Maslov's complex germ
General electromagnetic fields

Vortex electrons

Bliokh et al.

$\psi \propto e^{il\varphi}$

Microscope experiments

Uchida–Tonomura
Verbeeck et al.
McMorran et al.

Vortex-state transport became experimentally accessible.

Bagrov et al., TMP (1982), Ann. Phys. (1996), Dirac theory (1998), review (2000)
Bliokh et al., PRL (2007) Uchida–Tonomura, Nature (2010) Verbeeck et al., Nature (2010) McMorran et al., Science (2011)

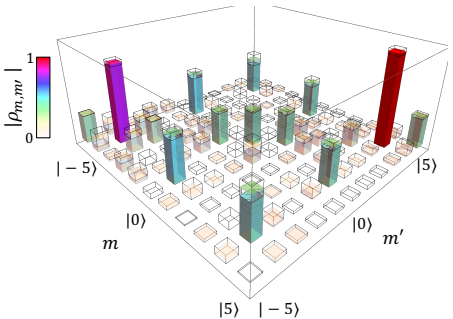
Quantum tomography: populations and coherence

Electron microscopy: 300 keV

Several analyser settings

ρ_{mm}
OAM probabilities

$\rho_{mm'} \quad (m \neq m')$
Coherence between modes



OAM reconstruction with physical constraints

MeV goal: reconstruct the state before and after transport.

Tavabi et al., arXiv:2607.29565 (2026), Fig. 2C. The plotted matrix describes the measured OAM subspace.